



Direct Shear Test for Coarse Granular Soil

Katarzyna Dołżyk-Szypcio¹

Received: 2 September 2018 / Revised: 17 February 2019 / Accepted: 27 February 2019 / Published online: 12 March 2019
© The Author(s) 2019

Abstract

A large direct shear apparatus was used to test coarse granular soil. In shear tests with a small shear box, deformation in shear band is homogeneous and stress–dilatancy relationships at pre-peak and post-peak phases of shearing are similar. However, in tests with a large shear box, the pre-peak and post-peak stress–dilatancy relationships are different. Using frictional state theory, it has been shown that the stress–dilatancy relationship for the large shear box is different from that for the small one conventionally used in direct shear tests, which suggests higher non-homogeneity deformation in the shear band in a large shear box in comparison to that in a small one. Parameter α of frictional state theory equals zero for the small and large shear boxes at failure. Parameter $\beta = 1.4$ for the small shear box and is a function of initial moisture and compaction for the large shear box. Average values of β range between 2.27 and 2.52 for dry coarse granular soil and between 2.17 and 2.30 for wet one. The value of critical frictional state angle $\Phi^\circ = 41.2^\circ$ of tested coarse granular soil is independent of soil moisture and compaction. The influence of the box's size on stress–dilatancy relationship has also been observed in the previous studies.

Keywords Large direct shear · Dilatancy · Frictional state · Coarse granular soil · Stress–dilatancy

List of Symbols

| | |
|----------------------|--|
| d_{50} | Mean grain diameter |
| C_u | Uniformity coefficient |
| C_c | Coefficient of curvature |
| ρ_{dmax} | Maximum dry density for standard compaction test |
| ρ_d | Dry density |
| D_c | Degree of compaction |
| w | Moisture (water content) |
| τ | Shear stress in shear plane |
| σ_n | Normal stress in shear plane |
| θ | Lode angle for stress |
| θ_ϵ | Lode angle for plastic strain increment |
| η | Stress ratio |
| α, β | Parameters of frictional state theory |
| D | Dilatancy |
| $\delta s, \delta h$ | Increments of displacement and sample height |
| Φ_r | Angle of friction at residual state |

| | |
|--------------|---|
| Φ° | Critical frictional state angle |
| Φ_{cv} | Critical state angle of shearing resistance |

1 Introduction

A typical flexible road pavement structure consists of different layers. Immediately below the bituminous surface layers are at least two more layers: first, a base course made of granular material and second, a sub-base usually made of a granular material with lower quality, higher fines content, and poorer grading than the base course material. Beneath the sub-base, the upper surface of fill or virgin ground is usually considered another layer, known as the subgrade [1].

The strength of the coarse granular material used as sub-base road material may be determined in a large direct shear test. In Poland, the maximum grain size of granular materials used for the base and sub-base layers is usually 31.5 mm. Therefore, the minimum diameter of the sheared sample has to be ten times the maximum particle diameter (315 mm) and the initial specimen height must be at least six times the particle diameter (189 mm) [2]. Thus, ordinary direct shear devices cannot be used.

Different triaxial and direct shear apparatuses have been constructed for testing coarse materials [e.g., 2–7]. A new large direct shear apparatus was constructed at Białystok

✉ Katarzyna Dołżyk-Szypcio
k.dolzyk@pb.edu.pl

¹ Department of Geotechnics and Structural Mechanics, Faculty of Civil and Environmental Engineering, Białystok University of Technology, ul. Wiejska 45E, 15-351 Białystok, Poland

University of Technology. Samples with a diameter of 500 mm and a height of 310 mm may be directly sheared with different displacement velocities. The horizontal force and changes of the sample height during shear can be automatically measured and continuously recorded by a computer.

The stress–dilatancy relationship is an important soil property. The most widely known relations are Taylor's [8] and Bolton's [9]. The general stress–dilatancy relationships for different deformation modes have been developed by Szypcio [10].

This paper presents the direct shear results for coarse-grained soil as typical sub-base road material in Poland at two moisture contents and three levels of compaction. Especially, the stress–dilatancy relationships are analysed in detail and demonstrated as being different for pre-peak and post-peak deformations. This is not observed in ordinary direct shear test of sands [8, 11]. The non-homogeneity of deformation in a shear band for a large direct shear is higher than for a smaller one, and this influences the stress–dilatancy relationship [2, 12–14].

It is shown that the strength of the tested material is a function of the dilatancy angle developed by Bolton [9]. Taylor's formula [8] underestimated the strength of the tested material in a large direct shear box.

2 Material Tested

The tested coarse granular material is typically used for the construction of the sub-base course of flexible road pavements in Poland. The gradation of this material is shown in Fig. 1.

The tested material is a 0/31.5 multi-graded aggregate with a maximum grain size of 31.5 mm with about 2% of the particles being smaller than 0.063 mm. The mean grain diameter is $d_{50} = 4.9$ mm, the uniformity coefficient is $C_u = 24$, and the coefficient of curvature is $C_c = 1.43$. In

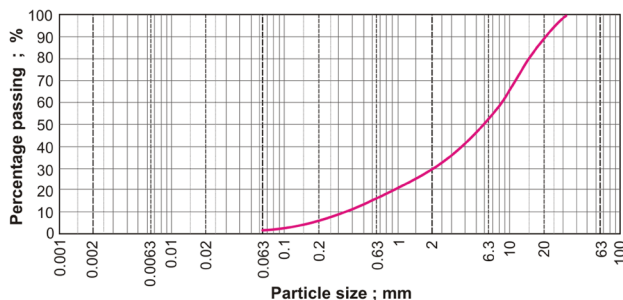


Fig. 1 Grain size distribution curve

general, the material is obtained from natural deposits by

extraction. This material is sieved and newly formed with some crushed material added.

In the tested material, about 25% of the gravel fraction consists of crushed grains. A compaction test was conducted in accordance with BS 1377: Part 4:1990, with compaction energy of 0.6 MNm/m^3 . The relationship between dry density and water content is shown in Fig. 2. The maximum dry density is $\rho_{d \max} = 2.249 \text{ g/cm}^3$ and the optimum water content is 6.2%. A similar relationship was obtained for different gravels [15].

3 Large Direct Shear Device

A schematic diagram and photo of the large direct shear apparatus constructed at Bialystok University of Technology are shown in Fig. 3.

A massive steel base platform with roller bearings moves

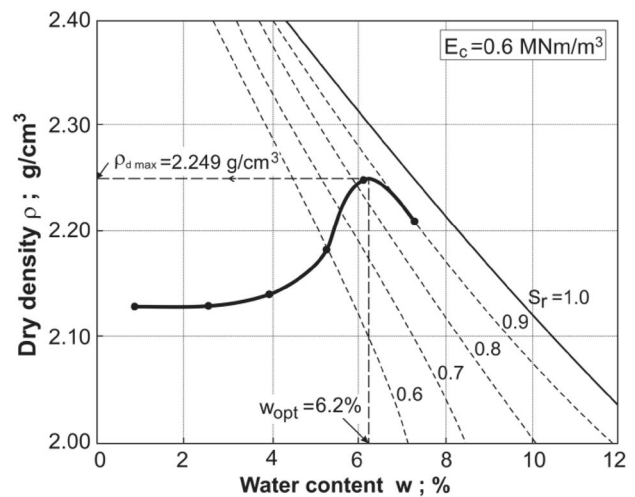


Fig. 2 Normal compaction test results

on a track. The roller bearings minimise friction. On the platform, a large-diameter cylindrical split box is mounted. The inner steel base of the box has a rough surface. The inner vertical surface of the box is polished to minimise friction between the soil and steel. The upper and lower parts of the box are clamped during sample preparation and consolidation. After sample preparation, a rigid plate with a rough bottom surface connected to a piston is placed on the levelled surface of soil. A project vertical force was hydraulically applied to the sample. An accuracy of a vertical force value was 0.1 kN. After vertical loading, the sample was consolidated. After consolidation, the upper part of the shear box is slightly raised to eliminate friction between the upper and lower parts of the shear box during shear. The force transferred onto the sample is automatically measured and

held constant during the shear. On the plate, three vertical displacement electronic transducers are mounted. During shear, the vertical displacement of the plate and changes of sample height are constantly measured and recorded on a computer. During shear, the upper half of the large shear box is maintained in a stable position by two tension ties. The tension ties are connected to the massive base (Fig. 3) and upper half of the shear box. The long ties are positioned precisely at the level of the shear plane and do not cause additional vertical force during shear [14]. The tension rod, horizontally positioned in the shear plane [14], pulls the lower part of the large shear box with a constant velocity of 1 cm/min. The horizontal displacement of force is automatically measured constantly and the measurements are recorded on a computer.

The friction between the platform and base was calibrated (Fig. 4).

As expected, the relationship between friction force T^* and normal force N is almost linear and expressed by the following equation:

$$T^* = 2.07 + 0.1130 \cdot N, \tag{1}$$

where T^* and N are expressed in kilonewtons.

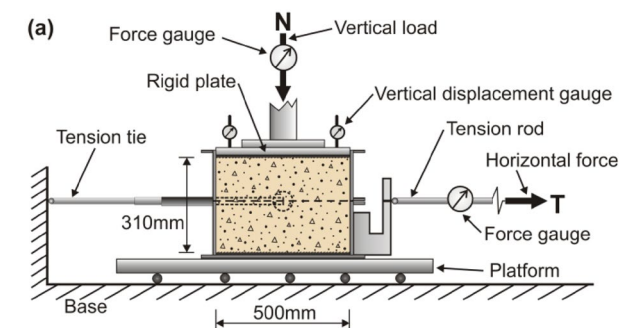


Fig. 3 Large direct shear device: a schematic diagram and b photos of the large direct shear box

4 Methodology

The tests were conducted at two moisture contents, three degrees of compaction, and three normal stresses (Table 1). The moisture content $w = 0.95\%$ in the air-dry state of the material under normal laboratory conditions and $w = 6.9\%$ is about a 0.7% higher moisture level than $w_{opt} = 6.2\%$.

The material was placed in the shear box in three equal layers. Each layer was compacted with constant compaction energy. A cylindrical steel hammer with mass of 10 kg and diameter of 12 cm was dropped from a constant height of 50 cm an appropriate number of times. The maximum, mean, and minimum level of compaction was obtained by a different number of hammer blows; that is, 30, 15, and 10, respectively, for each layer. The three levels of compaction were obtained for each moisture content as a function of used compaction energy. The mean values of compaction energy for the whole sample preparation were about 0.2, 0.1, and 0.07 MNm/m³, which is 0.3, 0.15, and 0.10, respectively, of the energy used in normal Proctor compaction tests [1, 15]. The degree of compaction obtained using this method of sample preparation was $D_c (=93\%, 90\%, \text{ and } 87\%)$ for air-dry sample $w = 0.95\%$ and $D_c (=98\%, 94\%, \text{ and } 90.5\%)$ for moisture sample $w = 6.9\%$, respective to the compaction energy used (Table 1). Therefore, the material compacted well and a relatively small compaction energy gave a relatively high degree of compaction.

After compaction, the sample surface was levelled, smoothed, and loaded. The forces transferred from the hydraulic system by a piston and plate on the sample were about 10, 25, and 50 kN to give normal stresses of 55.5–59.6 kPa, 130.9–133.9 kPa, and 254.6–258.2 kPa, respectively (Table 1). After load application, samples were consolidated by holding the load for 10 min. After consolidation, three vertical displacement transducers were mounted on the plate (Fig. 1), and the upper part of the shear

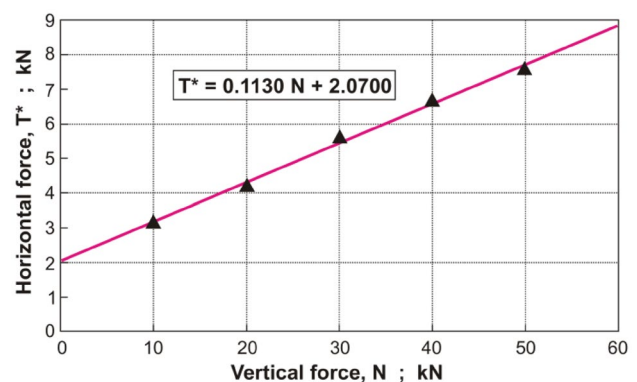


Fig. 4 Calibration of friction between the platform and base

Table 1 Parameters of the shear tests

| Test no. | Moisture w (%) | Compaction D_c (%) | Vertical stress σ_n (kPa) | Parameters | | | | | | |
|----------|------------------|----------------------|----------------------------------|------------------|----------------|---------------|----------------|---------------|---------------------|--------------------|
| | | | | Φ° (°) | α_1 (–) | β_1 (–) | α_2 (–) | β_2 (–) | α_{2avg} (–) | β_{2avg} (–) |
| 1 | 0.95 | 87 | 58.1 | 41.2 | 0.28 | 3.00 | 0.00 | 1.40 | 0.00 | 2.27 |
| 2 | | | 133.9 | | 0.30 | 5.00 | 0.00 | 3.20 | | |
| 3 | | | 258.2 | | 0.10 | 2.50 | 0.00 | 2.20 | | |
| 4 | | 90 | 59.6 | | 0.50 | 3.50 | 0.00 | 2.70 | 0.00 | 2.52 |
| 5 | | | 132.2 | | – | – | – | – | | |
| 6 | | | 258.7 | | 0.10 | 2.30 | 0.00 | 2.35 | | |
| 7 | | 93 | 57.0 | | 1.10 | 4.50 | 0.00 | 2.60 | –0.03 | 2.33 |
| 8 | | | 131.9 | | 0.40 | 2.80 | 0.00 | 2.20 | | |
| 9 | | | 257.2 | | –0.10 | 2.20 | –0.10 | 2.20 | | |
| 10 | 6.9 | 90.5 | 56.0 | | 0.10 | 2.10 | 0.00 | 1.90 | 0.00 | 2.30 |
| 11 | | | 130.9 | | 0.10 | 2.30 | 0.00 | 2.20 | | |
| 12 | | | 254.6 | | 0.00 | 2.80 | 0.00 | 2.80 | | |
| 13 | | 94 | 56.5 | | 0.25 | 2.50 | 0.00 | 2.05 | 0.00 | 2.17 |
| 14 | | | 132.4 | | 0.50 | 3.50 | 0.00 | 2.10 | | |
| 15 | | | 255.2 | | 0.80 | 6.00 | 0.00 | 2.35 | | |
| 16 | | 98 | 55.5 | | 0.40 | 3.00 | 0.00 | 2.25 | 0.00 | 2.27 |
| 17 | | | 131.4 | | 1.00 | 5.00 | 0.00 | 2.35 | | |
| 18 | | | 257.2 | | 0.35 | 3.20 | 0.00 | 2.20 | | |

box was raised about 0.5 mm to eliminate friction between the lower and the upper parts of the shear box during shear.

The tension tie holding the upper part of the shear box in a stable position and the tension rod transferring horizontal force to the lower part of the shear box were levelled in the shear plane and then shearing started. A velocity of displacement of 10 mm/min was used for all the tests. The vertical and horizontal forces and displacements were automatically registered and recorded on a computer. All tests were interrupted at a horizontal displacement of 60 mm (i.e., about 12% of the sample diameter).

5 Test Results

The results of the shear tests are shown in Figs. 5 and 6. The results of the shear test sample with $w=0.95\%$ and $\sigma_n=134$ kPa are not shown, because the plate was strongly tilted and changes of the sample height during shear could not be directly calculated.

6 Stress–Dilatancy for Direct Shear

The stress–dilatancy relationship for direct shear developed by Szypcio [11] is as follows:

$$\frac{\tau}{\sigma_n} = \frac{\sqrt{3}\eta \cos \Phi^\circ \cos \theta}{3 + \eta(\sin \theta - \sqrt{3} \sin \Phi^\circ \cos \theta)}, \quad (2)$$

where:

$$\eta = Q - AD, \quad (3)$$

$$Q = M^\circ - \alpha A^\circ, \quad (4)$$

$$M^\circ = \frac{3 \sin \Phi^\circ}{\sqrt{3} \cos \theta - \sin \Phi^\circ \sin \theta}, \quad (5)$$

$$A^\circ = \frac{1}{\cos(\theta - \theta_\epsilon)} \left\{ 1 - \frac{2}{3} M^\circ \sin(\theta + \frac{2}{3}\pi) \right\}, \quad (6)$$

$$A = \beta A^\circ, \quad (7)$$

$$\theta_\epsilon = \arctan \left\{ \frac{1}{\sqrt{3}} \frac{\delta h / \delta s}{\sqrt{1 + (\delta h / \delta s)^2}} \right\}, \quad (8)$$

$$D = -\sqrt{3} \frac{\delta h / \delta s}{\sqrt{1 + \frac{4}{3}(\delta h / \delta s)^2}}, \quad (9)$$

where Φ° is the critical frictional state angle, and α and β are the parameters of frictional state theory. For direct shear, as a special case of plane strain conditions (biaxial compression), the Lode angle for stress may be assumed to be $\theta=15^\circ$ [11, 16], h is the growth of sample height during

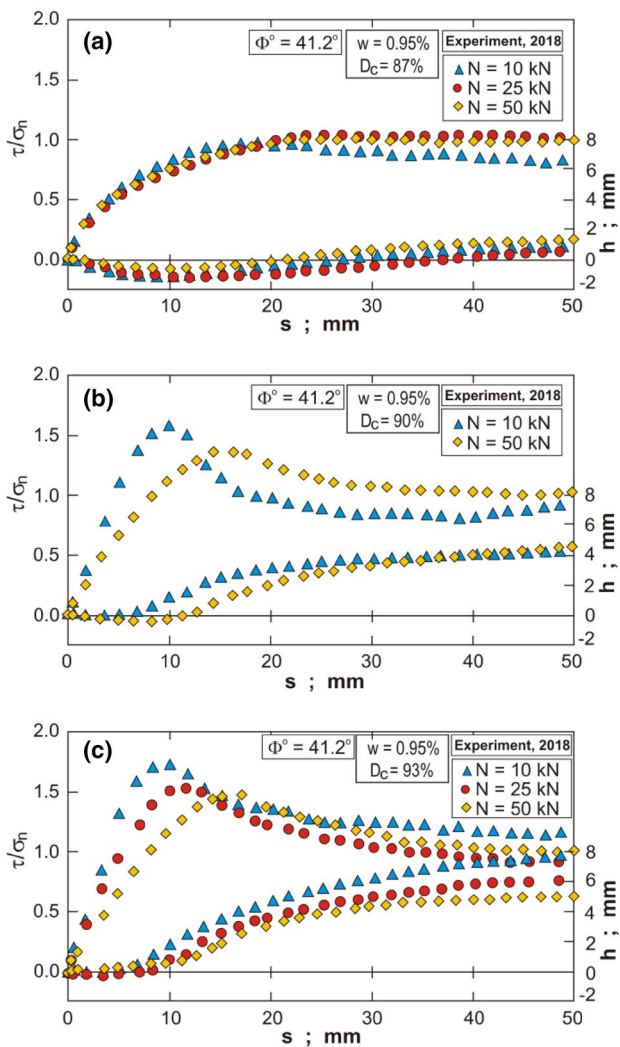


Fig. 5 Direct shear test results for air-dry soil: a $D_c=87\%$, b $D_c=90\%$, and c $D_c=93\%$

shear, and s is the displacement of the lower part of the shear box. An example of the stress–dilatancy relationship is shown in Fig. 7.

The shear stress is calculated by the following equation:

$$\tau = \frac{T - T^*}{A}, \tag{10}$$

where T is the horizontal force transferred by the tension rod, T^* is friction force between the platform and the base calculated by Eq. (1), and $A=0.19635 \text{ m}^2$ is the sample section area. The normal stress is as follows:

$$\sigma_n = \frac{N}{A}, \tag{11}$$

where N is the vertical force transferred to the sample.

The critical frictional state angle (Φ°) is the angle at critical state ($\delta h/\delta s = 0$) for granular soils [11] independent

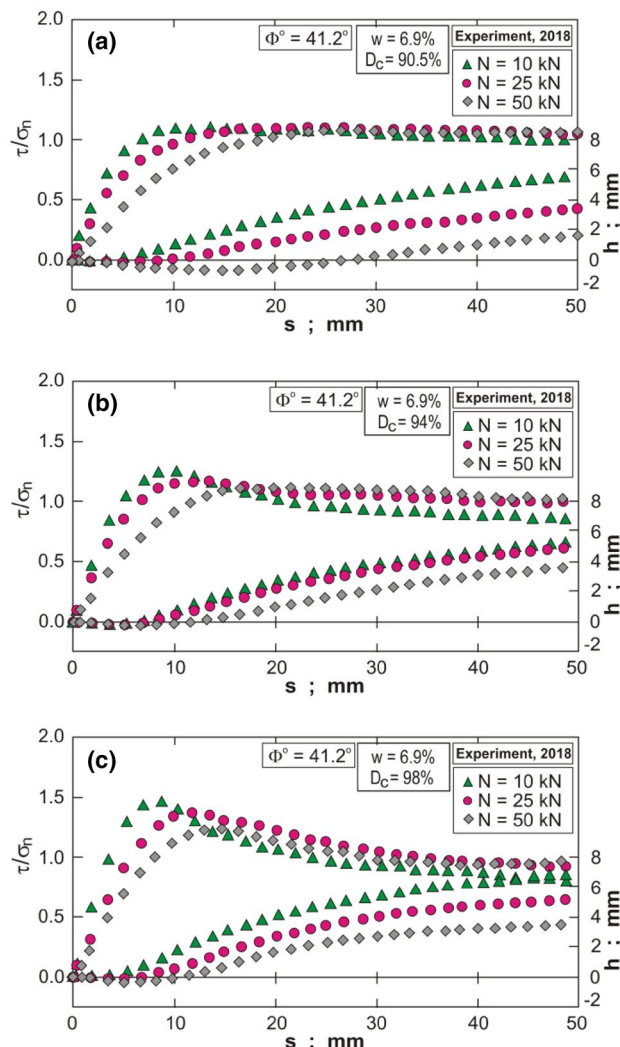


Fig. 6 Direct shear test results for moisture soil: a $D_c=90.5\%$, b $D_c=94\%$, and c $D_c=98\%$

of the initial compaction and water content of the soil. For the tested coarse granular soil, $\Phi^\circ=41.2^\circ$. The parameters α and β represent the mode of deformation [11, 16] and the level of soil destructuration in the shear band. For almost all tests, at the initial phase of shearing, the relationship between τ/σ_n and $\delta h/\delta s$ was not linear and parameters α and β cannot be accurately calculated. In later (pre-peak and post-peak) phases of shearing, the linear relationship $\tau/\sigma_n - \delta h/\delta s$ was observed, and parameters α and β can be calculated by use of an approximation technique. In this study, the least-squares method was used and the values of α_1, β_1 and α_2, β_2 for pre-peak and post-peak phases of shearing, respectively, are calculated and shown in Table 1. Note that using a different approximation method may produce slightly different values of these parameters [17, 18].

Using the small size box for direct shear, identical pre-peak and post-peak relationships between τ/σ_n and $\delta h/\delta s$

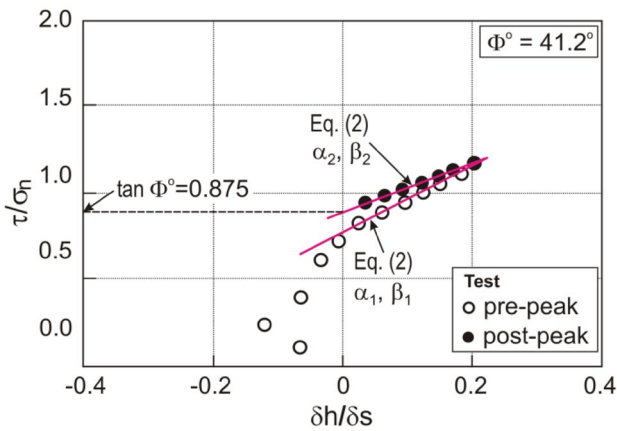


Fig. 7 Example of stress–dilatancy relationship

were obtained and $\alpha=0, \beta=1.4$ [16]. This proves that higher non-homogeneity deformation in the shear band is in the large box apparatus, compared with the small one.

The stress–dilatancy relationships for all tests are shown in Figs. 8 and 9.

Figures 8, 9 show only the average theoretical stress–dilatancy relationships for the peak and post-peak phases of shearing defined by Eq. (2) with $\alpha = \alpha_{2avg}$ and $\beta = \beta_{2avg}$.

For direct shear, Taylor’s stress–dilatancy relationship has [8] the following form:

$$\frac{\tau}{\sigma_n} = \tan \Phi_r + \frac{\delta h}{\delta s}, \tag{12}$$

where Φ_r is the angle of friction at the residual state. It may be assumed that $\Phi_r = 41.2^\circ$ for the tested material.

Bolton’s equation has the following form:

$$\tan \Phi = \tan \Phi_{cv} + 0.8\Psi_{max}, \tag{13}$$

where Φ is the angle of friction at failure, $\Phi_{cv} = \Phi^\circ = 41.2^\circ$ [10, 16], and the dilatancy angle at failure is as follows:

$$\Psi_{max} = \arctan \left(\frac{\delta h}{\delta s} \right)_{max}. \tag{14}$$

Figure 10 shows the stress–dilatancy relationships for the failure states.

Equation (2) obtained from frictional state theory well approximates the experimental relationship at failure for $\Phi^\circ = 41.2^\circ, \alpha=0$, and $\beta=2.2$. Bolton’s relation (13) also gives a relatively good approximation. For the experimental maximum dilatancy $(\delta h/\delta s)_{max}$, the maximum shear ratio $(\tau/\sigma_n)_{max}$ calculated by Taylor’s Eq. (12) is significantly smaller than that obtained from experiment. For tests in the small direct shear apparatus, Taylor’s relationship (12) is correct [8, 11]. Therefore, Eq. (2) is correct for tests in the small direct shear apparatus with $\alpha=0$ and $\beta=1.4$ [11]. In the author’s opinion, the source of this fact is the large size of the direct shear box

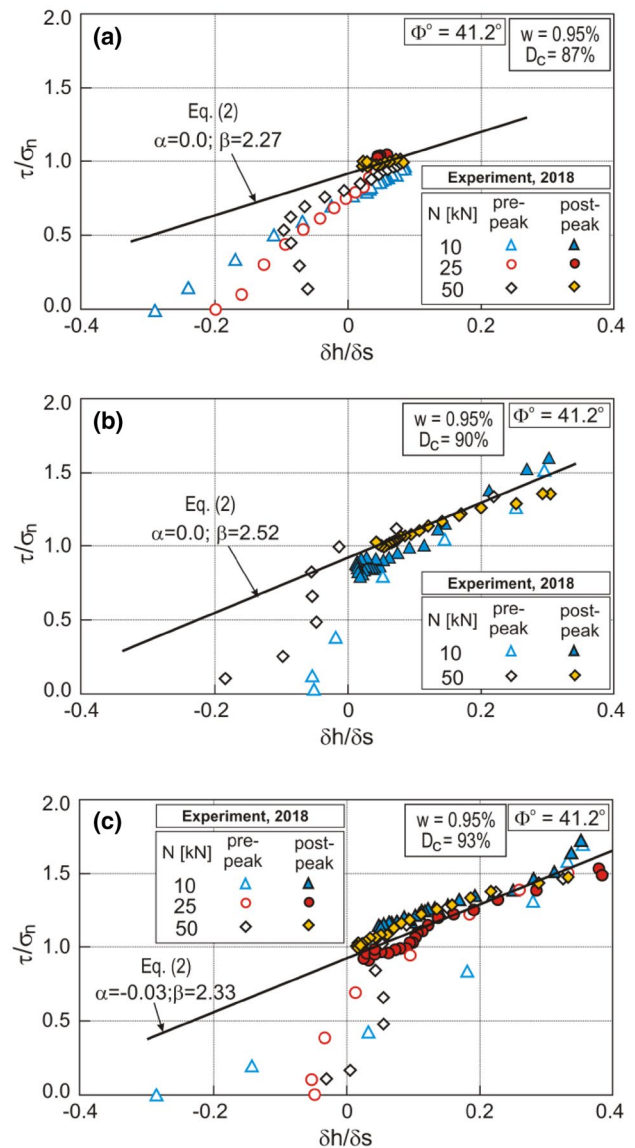


Fig. 8 Stress–dilatancy relationships for direct shear of air-dry soil: a $D_c = 87\%$, b $D_c = 90\%$, and c $D_c = 93\%$

used in the tests. The non-homogeneity of deformation in the shear band is higher in the large shear box apparatus than in the small one. Thus, the size of the direct shear apparatus influences the stress–dilatancy relationship [4, 11, 19].

7 Conclusions

A large direct shear apparatus can be used for testing coarse granular materials.

The stress–dilatancy relationship is a function of moisture, degree of compaction, and normal stresses. Taylor’s stress–dilatancy relationship is not correct for tests in a large direct shear apparatus. The stress–dilatancy relationships

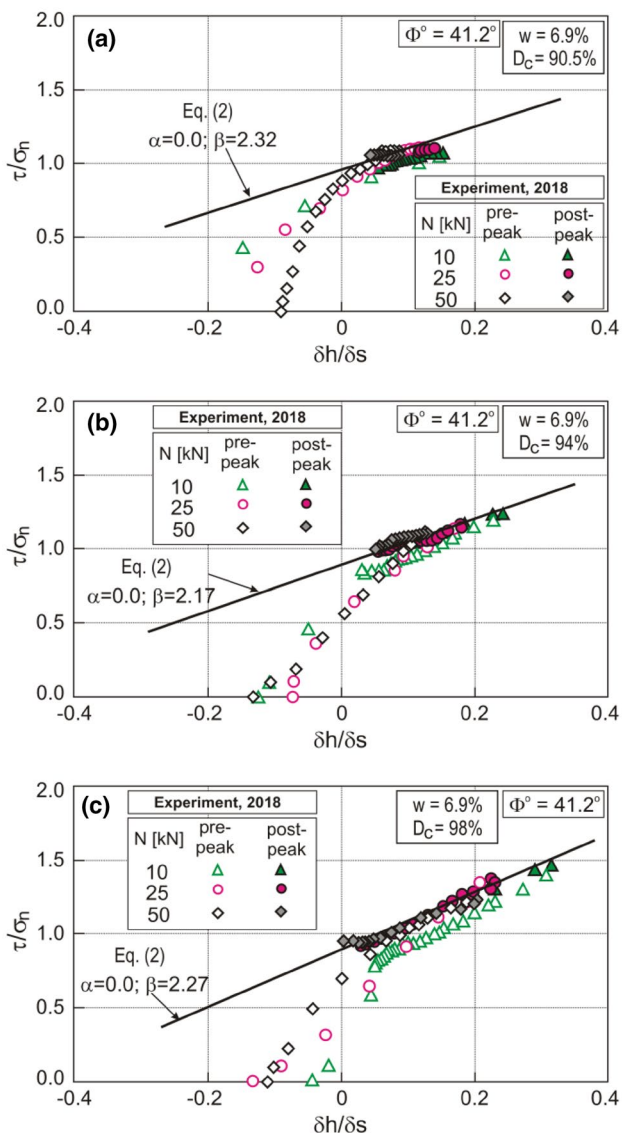


Fig. 9 Stress–dilatancy relationships for direct shear of moisture soil: **a** $D_c = 90.5\%$, **b** $D_c = 94\%$, and **c** $D_c = 98\%$

obtained from frictional state theory and Bolton’s theory are correct for the peak and post-peak phase of shearing.

Contrary to tests in a small direct shear apparatus, the parameters α and β in a large apparatus are different for the pre-peak and post-peak phases of shearing.

Open Access This article is distributed under the terms of the Creative Commons Attribution 4.0 International License (<http://creativecommons.org/licenses/by/4.0/>), which permits unrestricted use, distribution, and reproduction in any medium, provided you give appropriate credit to the original author(s) and the source, provide a link to the Creative Commons license, and indicate if changes were made.

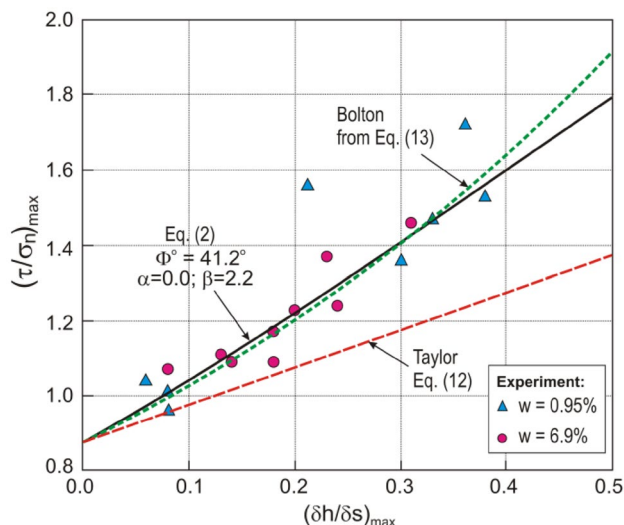


Fig. 10 Relationship between $(\tau/\sigma_n)_{max}$ and $(\delta h/\delta s)_{max}$

References

- Rodriguez AR, Castillo HD, Sowers GF (1988) Soil mechanics in highway engineering. Trans Tech Publications, Clausthal-Zellerfeld
- Bareither CA, Benson CH, Edil TB (2008) Comparison of shear strength of sand backfills measured in small-scale and large-scale direct shear tests. *Can Geotech J* 45(9):1224–1236. <https://doi.org/10.1139/T08-058>
- Lings ML, Dietz MS (2004) An improved direct shear apparatus for sand. *Géotechnique* 54(4):245–256. <https://doi.org/10.1680/geot.2004.54.4.245>
- Cerato AB, Lutenege AJ (2006) Specimen size and scale effects of direct shear box tests of sands. *ASTM Geotech Test J* 29(6):507–516. <https://doi.org/10.1520/GTJ100312>
- Liu SH (2009) Application of in situ direct shear device to shear strength measurement of rockfill materials. *Water Sci Eng* 2(3):48–57. <https://doi.org/10.3882/j.issn.1674-2370.2009.03.005>
- Nakao T, Fityus S (2008) Direct shear testing of a marginal material using a large shear box. *ASTM Geotech Test J* 31(5):393–403. <https://doi.org/10.1520/GTJ101237>
- Dissanayake DMAGB, Kurukulasuriya LC, Dissanayake PBR (2016) Evolution of shear strength parameters of rail track ballast in Sri Lanka. *J Natl Sci Found Sri Lanka* 44(1):61–67. <https://doi.org/10.4038/jnsf.v44i1.7982>
- Taylor DW (1948) *Fundamentals of soil mechanics*. Wiley, New York
- Bolton MD (1986) The strength and dilatancy of sands. *Géotechnique* 36(1):65–78. <https://doi.org/10.1680/geot.1986.36.1.65>
- Szypcio Z (2016) Stress–dilatancy for soils. Part I. The frictional state theory. *Stud Geotech Mech* 38(4):51–57. <https://doi.org/10.1515/sgem-2016-0030>
- Szypcio Z (2017) Stress–dilatancy for soils. Part IV: experimental validation for simple shear conditions. *Stud Geotech Mech* 39(1):81–88. <https://doi.org/10.1515/sgem-2017-0008>
- Moayed RZ, Alibolandi M, Alizadeh A (2017) Specimen size effects on direct shear test of silty sands. *Int J Geotech Eng* 11(2):198–205. <https://doi.org/10.1080/19386362.2016.1205166>
- Wu PK, Matsushima K, Tatsuoka F (2008) Effects of specimen size and some other factors on the strength and deformation of

- granular soil in direct shear tests. *ASTM Geotech Test J* 31(1):45–64. <https://doi.org/10.1520/GTJ100773>
14. Jewell RA (1989) Direct shear tests on sand. *Géotechnique* 39(2):309–322. <https://doi.org/10.1680/geot.1989.39.2.309>
 15. Tatsuoka F (2011) Laboratory stress–strain tests for developments in geotechnical engineering research and practice. In: Chung CK, Kim HK, Lee JS, Jung YH, Kim DS (eds) *Deformation characteristics of geomaterials*. Proceedings of the 5th international symposium on deformation characteristics of geomaterials (IS), Seoul, Korea, September 2011. IOS Press, Amsterdam, pp 3–50. <https://doi.org/10.3233/978-1-60750-822-9-3>
 16. Szypcio Z (2017) Stress–dilatancy for soils. Part III: experimental validation for the biaxial condition. *Stud Geotech Mech* 39(1):73–80. <https://doi.org/10.1515/sgem-2017-0007>
 17. Das SK, Basudhar PK (2006) Comparison study of parameter estimation techniques for rock failure criterion models. *Can Geotech J* 43(7):764–771. <https://doi.org/10.1139/t06-041>
 18. Das SK, Basudhar PK (2009) Comparison of intact rock failure criteria using various statistical methods. *Acta Geotech* 4(3):223–231. <https://doi.org/10.1007/s11440-009-0088-1>
 19. Xiao Y, Liu H, Zhang W, Liu H, Yin F, Wang Y (2016) Testing and modelling of rockfill materials: a review. *J Rock Mech Geotech Eng* 8(3):415–422. <https://doi.org/10.1016/j.jrmge.2015.09.009>